

Registration of Dynamic Contrast Enhanced MRI with Local Rigidity Constraint

Lars Ruthotto¹, Erlend Hodneland^{2,3}, and Jan Modersitzki¹

¹ Institute of Mathematics and Image Computing, University of Lübeck, Germany

² Department of Biomedicine, University of Bergen, Norway

³ Department of Radiology, Haukeland University Hospital, Bergen, Norway

lars.ruthotto@mic.uni-luebeck.de

<http://www.mic.uni-luebeck.de>

Abstract. Dynamic Contrast Enhanced Magnetic Resonance Imaging (DCE-MRI) of the kidney provides important information for the diagnosis of renal dysfunction. To this end, a time series of image volumes is acquired after injection of a contrast agent. The interpretation and pharmacokinetic analysis of the time series data is highly sensitive to motion artifacts. Registration of these data is a challenging task as contrast uptake adds new image features and gives rise to intensity changes over time within the kidneys.

This paper presents a new registration pipeline for a time series of 3D DCE-MRI. The pipeline combines state-of-art modules such as a weighted and robust least squares type distance measure, a regularization that is based on hyperelasticity and thus ensures diffeomorphic transformations and enables the incorporation of local rigidity constraints on the kidneys. We provide results that indicate the necessity of these constraints and illustrate the superiority of the proposed pipeline as compared to other approaches.

Keywords: DCE-MRI, Motion Correction, Constrained Image Registration, Local Rigidity, Hyperelastic Registration.

1 Introduction

Dynamic Contrast Enhanced Magnetic Resonance Imaging (DCE-MRI) of the kidney provides in vivo information about the Glomerular Filtration Rate (GFR). The GFR is an important measure of renal function and useful in the diagnosis of chronic kidney diseases. To this end, a small dose of contrast agent, gadolinium, is administered and a time series of three dimensional images is acquired. Although the images are partly acquired during breath hold the time series can be affected by inconsistencies between the respiratory phases at the instance of recording. Even small displacements can affect the voxelwise pharmacokinetic analysis yielding incorrect estimates of the GFR [8] and thus limit the usability of DCE-MRI. In particular, when looking at the uptake rate in the cortex of the kidneys, this is an important issue.

Registration of DCE-MRI time series is a challenging task since intensity changes in the region of interest take place due to uptake of bolus, but also from geometrical changes due to inconsistent breath hold, free breathing after breath hold, patient movements and physiological pulsations. New features may appear during wash in and disappear during the wash out phase, which can mislead unimodal distance measures.

DCE-MRI registration is an important challenge and has thus drawn much attention. Melbourne et al. [7] proposed a nonlinear registration scheme based on repeated registrations of the data to a reference time series generated by a Principal Component Analysis (PCA). The reference volumes preserve long term contrast uptake but show less motion. Their approach is based on the assumption that the displacements between acquisitions is periodically or random. Alternatively the impact of intensity variations on nonlinear registration schemes can be suppressed by multi-modal distance measures such as mutual information [13,14] or normalized gradient fields [4,6]. Under the assumption that uptake of contrast agent is limited to the kidneys the registration problem is essentially uni-modal in large parts of the image. This assumption is also supported by our analysis of the results for kidney data from Haukeland University Hospital, Bergen, Norway. Another option to gain robustness against uptake-induced intensity modulations is to limit the flexibility of the transformation model. A direct comparison between nonlinear and rigid transformation models on the entire image and limited to rectangular regions around the kidneys was performed in [11]. The results suggest that rigidity is useful to describe the motion of the kidneys, however, improper to model the overall respiratory motion [11].

In this paper, we propose a novel nonlinear registration pipeline with local rigidity constraints on the kidneys [12,5]. Thereby we ensure that the relevant contrast variations related to blood clearance are preserved in the registered time series. Further the robustness of the registration against intensity changes related to contrast uptake is improved. Our comparison with an unconstrained approach demonstrates the improvement that can be gained by integrating the local rigidity constraints. In contrast to [11], a globally smooth and nonlinear transformation is estimated and the registration is driven by a very robust uni modal distance measure. Smooth transitions between the constrained and unconstrained regions are provided by a novel hyperelastic regularizer [2]. This remarkable regularizer prohibits tissue folding and thus it is guaranteed to compute a diffeomorphic transformation independent of the choice of regularization parameters.

First promising results on clinical data are presented and suggest that local rigidity is a useful option to reduce the degradation of DCE-MRI due to motion artifacts.

2 Locally Rigid Registration Scheme

Given a time series of three dimensional images $\mathcal{I}_1, \dots, \mathcal{I}_T$ on a domain $\Omega \subset \mathbf{R}^3$ our goal is to eliminate the motion between the individual time points. To this end, we aim to register all image volumes to an assigned reference image – in the following

$\mathcal{R} := \mathcal{I}_1$. For ease of presentation, we limit the description to one subproblem, i.e. the registration of one arbitrary time frame $\mathcal{T} \in \{\mathcal{I}_2, \dots, \mathcal{I}_T\}$ to \mathcal{R} .

Since displacements due to respiratory motion on the entire thorax are nonlinear, we choose a non-parametric model for the mapping $y : \Omega \rightarrow \mathbf{R}^3$ [9].

In our application difficulties arise due to uptake related intensity variations within the kidneys. The goal is to preserve this essential piece of information, but nevertheless eliminate the displacement between the frames in the time series. As our analysis of the data indicates, the DCE-MRI registration problem is essentially unimodal outside the kidney regions. Therefore we choose a simple and robust weighted SSD distance measure

$$\mathcal{D}(\mathcal{T}, \mathcal{R}) := \frac{1}{2} \int_{\Omega} (\mathcal{T}(x) - \mathcal{R}(x))^2 v(x) dx. \quad (1)$$

The weighting function $v : \Omega \rightarrow \mathbf{R}^+$ is used to reduce the influence of regions with varying signal intensities, see Sec. 3 for details.

2.1 Locally Rigid Image Registration

To avoid misregistrations due to uptake induced contrast variations we aim to limit the flexibility of the transformation within the kidneys by adding rigidity constraints as motivated by [11].

Our notation and implementation follows [5]. Let $M_1, M_2 \subset \Omega$ denote the regions of the kidneys in the reference image \mathcal{R} . The idea is to restrict the nonlinear transformation y to be locally rigid on M_1 and M_2 . This motivates the formulation of the constrained registration problem [5]

$$\begin{aligned} \min_{y, w} \quad & \frac{1}{2} \int_{\Omega} (\mathcal{T}(y(x)) - \mathcal{R})^2 |\det \nabla y(x)| v(x) dx + \mathcal{S}[y] \\ \text{subject to} \quad & y(x) = Q(x)f(w_i) \quad \forall x \in M_i, i = 1, 2. \end{aligned} \quad (2)$$

Note the appearance of $|\det \nabla y(x)|$ due to a change of the coordinate system and the transformation rule; see [5] for details. As for the constraints, $Q(x)$ describes a model for a linear transformation, w_1 and w_2 are the six parameters of the rigid transformations for the two kidney regions and f is the embedding of the rigid space into the space of affine linear transformations; see [5] for details. The regularization \mathcal{S} is discussed in the next subsection.

2.2 Hyperelastic Regularization

To allow for large transformations and to enforce invertibility we choose a hyperelastic regularizer [2]

$$\mathcal{S}^{\text{hyper}}(y) = \alpha_l \mathcal{S}^{\text{length}}(y) + \alpha_a \mathcal{S}^{\text{area}}(y) + \alpha_v \mathcal{S}^{\text{volume}}(y). \quad (3)$$

This regularizer controls the changes in length, area and volume induced by the transformation y . Due to the growth behavior and since infinite energy is required to annihilate a volume element, $\mathcal{S}^{\text{hyper}}$ guarantees the invertibility of

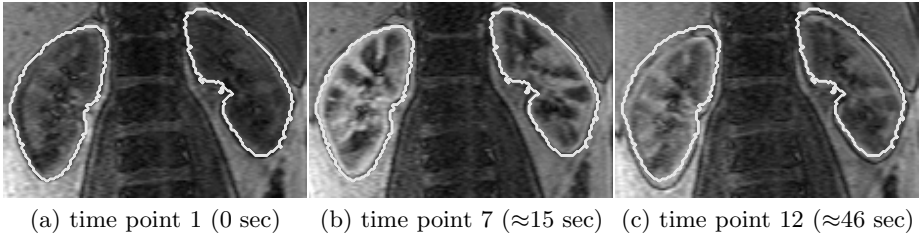


Fig. 1. Illustration of the motion problem in DCE-MRI. We exemplarily visualize three time points in coronal views. The semi automatic segmentation of the kidney obtained for the first image volume is represented by a white contour in (a) – (c). The appearance of new structures due to uptake of the contrast agent can for example be seen by comparing (a) to (b). The motion problem due to free breathing is observable for instance by comparing a) to (c).

the transformation even for large displacements and thus enforces diffeomorphic transformations. Moreover, the transformation field is very smooth and the hyperelastic regularizer is therefore especially attractive in combination with rigidity constraints to control volume changes in the neighborhood of the kidney cortices.

2.3 Numerical Implementation

The constrained registration algorithm is implemented using the publicly available toolbox FAIR in Matlab [9]. Important routines such as image interpolation, distance measures and hyperelastic regularizer are re-used. The problem is attacked in a multi-level strategy on a coarse-to-fine hierarchy of discretizations. Each discrete optimization problem is solved using a Newton-SQP optimizer [10]. The linear system is solved using a preconditioned minimum residual method [1] where the preconditioner is a slightly modified version of [3].

2.4 Test Data

A 1.5 Tesla MR-scanner (Avanto, Siemens) is used to acquire DCE-MRI data from a healthy volunteer. A breath-hold T1-weighted 3D single Gradient Recall Echo (GRE) pulse sequence was used to acquire signal-intensity time curves after administration of a small dose (2 ml) of gadolinium contrast media intravenously. The acquisition parameters for the examination was: Slice-thickness 3 mm, Repetition Time 3.3, Echo Time 1.79, Flip Angle 9, Acquisition Matrix 256×128 , Parallel factor 2, Time resolution is 2.5 sec in the breath hold phase (first 11 time frames) and 30 sec in the free breathing phase. The voxel size is $1.48 \times 1.48 \times 3$ mm.

The kidney segmentation in the first image volume $\mathcal{R} = \mathcal{I}_1$ that was delivered with the data was obtained using a semi-automatic segmentation using temporal curve information [6]. A training mask for each desired phase was given initially by the user, representative for the tissue classes to be found. Thus, a large set of

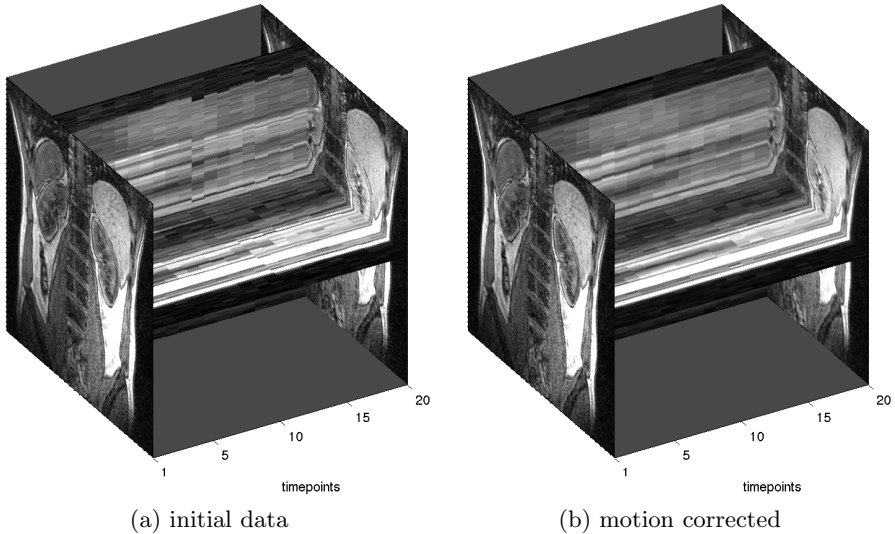


Fig. 2. 3D Motion correction results are visualized exemplarily for one coronal slice. The slice is shown at the first and last time point before (a) and after locally rigid registration (b). The time course is visualized by two planes. It is apparent, that the proposed scheme reduces motion artifacts as can be observed for example in the end of the breath hold at timepoint 11.

T -dimensional tissue vectors were obtained, where T is the number of time points. The algorithm uses the Mahalanobis distance between such temporal curve shapes to classify each voxel in space with KNN nearest-neighbor classification. Each voxel is assigned to the most abundant class within the K nearest neighbors in the training set. After classification, the voxel is assigned to the training set, and the algorithm runs iteratively until no voxels are changing class.

3 Results

We apply the proposed registration pipeline to the clinical data set consisting of 20 DCE-MRI image volumes. The template images $\mathcal{I}_2, \dots, \mathcal{I}_{20}$ are sequentially registered to the reference image \mathcal{I}_1 by solving the constrained registration problem (2). The distance measure (1) is weighted with arbitrarily chosen factors $v(x) = 0.05$ within the kidneys and $v(x) = 1$ elsewhere. For all 3D registration problems we use hand-picked regularization parameters, $\alpha_l = 300$, $\alpha_a = 30$, $\alpha_v = 300$, see (3).

The average reduction of the weighted distance measure \mathcal{D} (1) over all 19 registration problems is 48%. For all transformations the Jacobian determinant $\det \nabla y$ is in the interval $[0.43, 1.49]$ and hence, as guaranteed by our regularization scheme, all mappings are diffeomorphic.

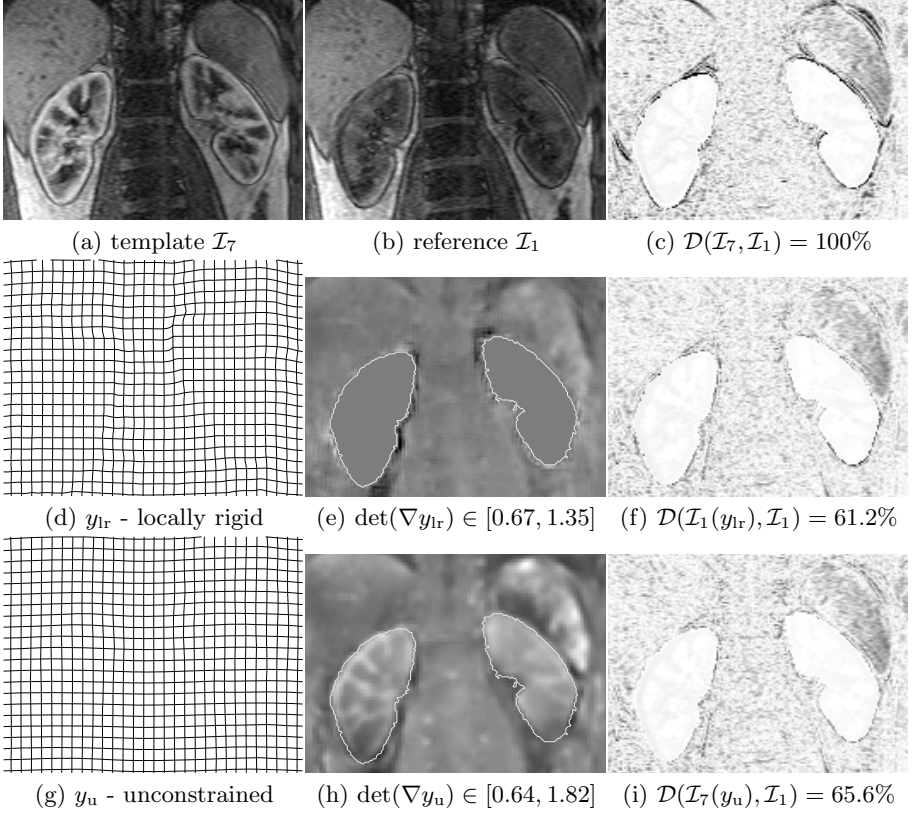


Fig. 3. Results of the 3D registration of the time points with most extreme variations in contrast uptake (\mathcal{I}_1 and \mathcal{I}_7) are visualized in one coronal slice. The template image \mathcal{I}_7 (a) is registered to the reference image \mathcal{I}_1 (b). The solutions of the registration with and without local rigidity constraints, y_r and y_u , are visualized in (d) and (g). Both transformations are smooth and diffeomorphic indicated by the Jacobian determinants being positive and finite (e) and (h). However, (h) also shows volumetric changes in the kidney regions which can be avoided using the constrained approach (e). A comparable reduction of the distance is achieved by both transformations, compare the absolute weighted distance images with identical colormap (c),(f) and (i).

Fig. 2 illustrates the considerable reduction of motion artifacts due to inconsistencies between the respiratory phases and free breathing as well as the improvement that can be gained using the proposed pipeline. The impact of the registration pipeline is illustrated exemplarily for one coronal slice. The time courses before and after locally rigid registration are visualized by two orthogonal planes in time dimension.

We exemplarily show more detailed results of the 3D registration for the images with the most extreme variations in contrast uptake (\mathcal{I}_1 and \mathcal{I}_7) in Fig. 3. We also demonstrate the importance of local rigidity constraints for this application by comparing the constrained with an unconstrained approach. In the

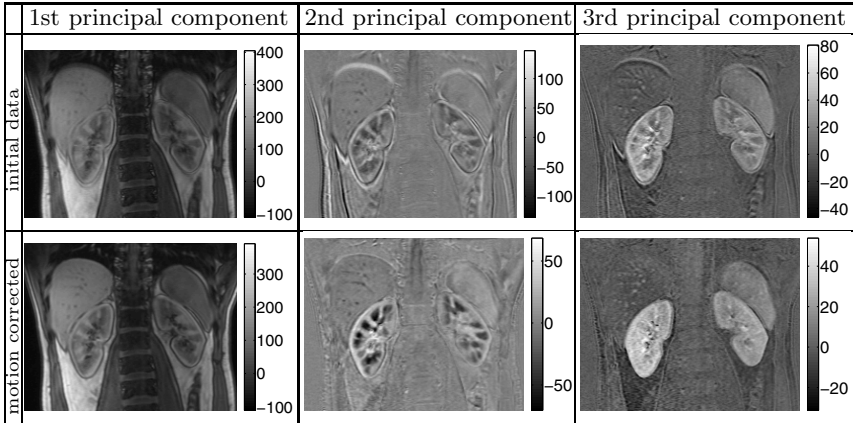


Fig. 4. 3D Results of Principal Component Analysis before (top row) and after registration (bottom row) are visualized exemplarily for one coronal slice. Projections of both datasets onto their first three principal components are shown. Artifacts due to inconsistent breath hold and free breathing manifest in all three projections of the initial data as shadows in the spleen, liver and kidney regions. The proposed correction scheme considerably reduced these artifacts, which manifests in reduced motion blur of the principal components. Note the considerable reduction of artifacts by the proposed registration approach as can be observed by reduced motion blur in the principal components.

unconstrained setting the regularization of volumetric changes are reduced by setting $\alpha_v = 0.01$. In both scenarios a comparable reduction in the difference images is achieved and essentially all structure outside the kidney regions vanishes, supporting our assumption that the registration problem is uni-modal outside the kidneys. Both transformations are very smooth and due to the hyperelastic regularizer also diffeomorphic. However, as to be expected the unconstrained registration introduces volumetric changes inside the kidneys to compensate the different uptake levels while the constrained scheme does not. Note that the underlying image differences relate to contrast uptake and not to tissue distortion. Hence the results of the constrained approach are superior.

As another indicator of the effectiveness of our method, we perform a Principal Component Analysis (PCA) of the time series before and after registration; see [7]. To this end, we remove the mean of each time point on the finest discretization level, compute the covariance matrices and their eigenvectors and eigenvalues. The projections onto the three principal components are shown in Fig. 4. The reduction of motion artifacts can be seen by comparing the respective projections. Before correction the first principal component is motion-blurred and contours of the spleen, liver and kidneys are shaded. Inconsistent respiratory phases and problems due to free breathing also manifest in the second and third principal component. After registration the first principal component is less blurred and the remaining projections describe the long term uptake behavior within the kidneys.

4 Discussion and Outlook

We present a novel image registration pipeline for Dynamic Contrast Enhanced MRI (DCE-MRI) of kidneys. The new pipeline combines a robust, weighted least squares based distance measure, a hyperelastic regularizer, and local rigidity constraints. The basic idea is to partition the domain into regions of primarily pharmacokinetic activities and remainder. In active regions tissue deformations are restricted to be locally rigid and thus uptake-induced intensity changes that are essential for pharmacokinetic analysis are preserved. The emphasis of the weighted distance measure is on the remainder, where the registration problem is approximately uni-modal. First promising results indicate that our pipeline considerably reduces motion artifacts related to inconsistencies between respiratory phases at the instance of recording and free breathing.

It is well known that unconstrained registration approaches may lead to incorrect changes of volume in kidneys. Synthetically generated reference images sharing the long term uptake behavior have been used to resolve this issue [7]. However, the synthesis is based on certain assumptions on the motion such as periodicity which can be questionable in acquisitions with breath hold and free breathing phases. We present experiments demonstrating that our new constrained approach is capable to register kidney DCE-MRI without making assumptions on the underlying motion.

Similar to [11] our findings suggest that local rigidity within the kidneys is a useful assumption to eliminate motion artifacts in DCE-MRI data related to respiration. Instead of computing separate rigid registrations of both kidneys as in [11], our scheme uses only one global transformation. Even though only the kidneys are of interest for the analysis of renal function, our experiments indicate that adjacent anatomical structures provide additional and useful information.

Our approach focuses on eliminating motion artifacts due to inconsistencies between respiratory phases at the instance of recording and free breathing. Further reasons for displacement between time frames such as physiological pulsations are not addressed. Obviously, our scheme is only indented for DCE-MRI of tissue where the local rigidity assumption holds. For DCE-MRI of tissue with severe non-rigid displacements our scheme may only serve as a rigid pre-registration step.

At present, the proposed scheme requires an initial segmentation of the kidneys in one reference image. In our case a semi automatic segmentation of the first time point was already provided with the data. In future work we will also investigate the integration of automatic kidney segmentations into our framework. We are positive that our scheme is robust against segmentation errors since the powerful hyperelastic regularization [2] gives a very smooth transition from the constrained to the unconstrained region.

Acknowledgements. We like to thank the *MR kidney function researchgroup* and Jarle Rørvik (MD, PhD) et al. from the Department of Surgical Sciences, University of Bergen and Department of Radiology, Haukeland University Hospital, Bergen, Norway for providing this interesting data. Furthermore we thank Åsmund Kjørstad for his segmentations of the kidneys.

References

1. Barrett, R.: Templates for the solution of linear systems. building blocks for iterative methods. Society for Industrial Mathematics (1994)
2. Burger, M., Modersitzki, J., Ruthotto, L.: A hyperelastic regularization energy for image registration. *SIAM Journal on Scientific Computing* (in revision) (2012)
3. Greif, C., Schötzau, D.: Preconditioners for saddle point linear systems with highly singular (1, 1) blocks. *Electronic Transactions on Numerical Analysis* 22, 114–121 (2006)
4. Haber, E., Modersitzki, J.: Intensity gradient based registration and fusion of multimodal images. *Methods of Information in Medicine* 46(3), 292–299 (2007)
5. Haber, E., Heldmann, S., Modersitzki, J.: A framework for image-based constrained registration with an application to local rigidity. *Linear Algebra and its Applications* 431, 459–470 (2009)
6. Hodneland, E., Kjørstad, A., Andersen, E., Monssen, J.A., Lundervold, A., Rørvik, J., Munthe-Kaas, A.: In vivo estimation of glomerular filtration in the kidney using DCE-MRI. In: *Image and Signal Processing and Analysis (ISPA)*, pp. 755–761. IEEE (2011)
7. Melbourne, A., Atkinson, D., White, M.J., Collins, D., Leach, M., Hawkes, D.: Registration of dynamic contrast-enhanced MRI using a progressive principal component registration (PPCR). *Physics in Medicine and Biology* 52(17), 5147–5156 (2007)
8. Michoux, N., Vallee, J., Pechere-Bertschi, A., Montet, X., Buehler, L., Van Beers, B.: Analysis of contrast-enhanced MR images to assess renal function. *Magnetic Resonance Materials in Physics, Biology and Medicine* 19(4), 167–179 (2006)
9. Modersitzki, J.: FAIR: Flexible algorithms for image registration (2009)
10. Nocedal, J., Wright, S.J.: Numerical optimization. Springer (1999)
11. Rogelj, P., Zöllner, F.G., Kovačič, S., Lundervold, A.: Motion correction of contrast-enhanced MRI time series of kidney. In: *Proceedings of the 16th International Electrotechnical and Computer Science Conference (ERK 2007)*, pp. 191–194 (2007)
12. Staring, M., Klein, S., Pluim, J.: A rigidity penalty term for nonrigid registration. *Medical Physics* 34, 4098 (2007)
13. Viola, P., Wells III, W.M.: Alignment by maximization of mutual information. *International Journal of Computer Vision* 24(2), 137–154 (1997)
14. Zöllner, F.G., Sance, R., Rogelj, P., Ledesma-Carbayo, M.J., Rørvik, J., Santos, A., Lundervold, A.: Assessment of 3D DCE-MRI of the kidneys using non-rigid image registration and segmentation of voxel time courses. *Computerized Medical Imaging and Graphics* 33(3), 171–181 (2009)